

Supporting Information

“Clickable” LNA/DNA Probes for Fluorescence Sensing of Nucleic Acids and Autoimmune Antibodies

*Anna S. Jørgensen, Pankaj Gupta, Jesper Wengel, and I. Kira Astakhova**

General	S2
Synthesis of monomer M ¹	S4
Chemical structures and photophysical characteristics of single molecule dyes used in this study (Table S1)	S8
Postsynthetic click chemistry	S9
IE HPLC retention times and MALDI MS of purified oligonucleotides (Table S2)	S11
UV-visible and thermal denaturation studies	S13
<i>T</i> _m values of the modified duplexes containing monomers M ² – M ⁵ compared to M ¹ -labelled references (Table S3)	S14
Effect of single-nucleotide mismatch on binding affinity and fluorescence sensing of DNA/RNA targets by ON7 and ON19 in a medium salt buffer (Table S4)	S15
<i>T</i> _m values of the modified duplexes containing monomers M ² – M ⁵ measured at the fluorophores' absorbance wavelength (Table S4)	S16
Ratio I/II of absorbance maxima of modified oligonucleotides and duplexes (Figure S5)	S17
Fluorescence studies	S19
Spectroscopic and photophysical properties of modified oligonucleotides and duplexes (Table S6)	S20
Representative fluorescence steady-state emission and excitation spectra (Figure S6)	S21
Autoantibody binding assay	S22
Fluorescence detection of antibody binding by single-stranded oligonucleotides and duplexes containing monomer M ² (Table S7)	S23
Molecular modeling of interactions between fluorescent probes and proteins used in this study	S24
Representative target titration curve (Figure S8)	S26

General

Reagents obtained from commercial suppliers were used as received. Phosphoramidite reagent **3** was prepared as described below (Scheme 1). Fluorescent azides and TBTA¹ for click chemistry were obtained from Lumiprobe LLC. 9,10-Diphenylanthracene (DPA), perylene, crezyl violete perchlorate and oxazine 170 used in spectral studies were recrystallized. HPLC grade light petroleum ether, methanol, ethanol, DCM and DMF were distilled and stored over activated 4Å molecular sieves. Other reagents and solvents were used as received. Photochemical studies were performed using spectroquality methanol, ethanol and cyclohexane.

Stock solutions for click chemistry were prepared as described.² Click reactions were performed in 1.5 mL eppendorf tubes (monomers **M**²–**M**⁴) or 1 mL reactor tubes (monomer **M**⁵) under argon using vigorous stirring in Emrys Creator (Personal Chemistry) in the latter case.

NMR spectra were recorded at 303 K on Bruker AVANCE III 400 MHz instrument. Chemical shifts are reported in ppm, relative to solvents peaks (DMSO-*d*₆: 2.5 ppm for ¹H and 39.5 ppm for ¹³C; 85% aq. H₃PO₄: 0.00 ppm for ³¹P). ¹H NMR coupling constants are reported in Hz and refer to apparent multiplicities. ESI high resolution mass spectra were recorded in positive ion mode using PE SCIEX QSTAR pulsar mass mass spectrometer. Analytical thin-layer chromatography was performed on Kieselgel 60 F254 precoated aluminium plates (Merck). Silica gel column chromatography was performed using Merck Kieselgel 60 0.040–0.063 mm. Silica gel (0.040-0.063 mm) used for column chromatography and analytical silica gel TLC plates 60 F254 precoated aluminium plates were purchased from Merck.

¹ Tris[(1-benzyl-1H-1,2,3-triazol-4-yl)methyl] amine (TBTA): T. R. Chan, R. Hilgraf, K. B. Sharpless, V. V. Fokin, *Org. Lett.*, 2004, **6**, 2853.

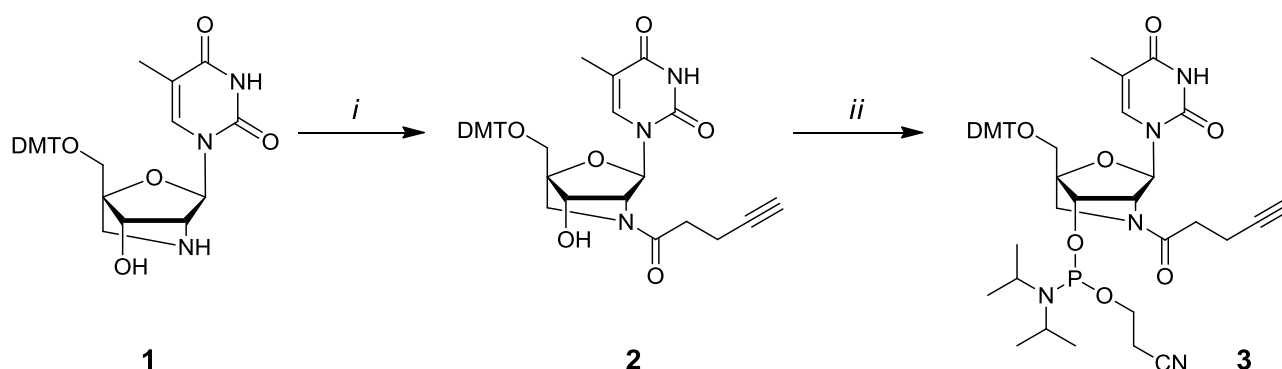
² Some reviews on DNA modification with click chemistry: a) A. V. Ustinov, I. A. Stepanova, V. V. Dubnyakova, T. S. Zatsëpin, E. V. Nozhevnikova, V. A. Korshun, *Russ. J. Bioorg. Chem.*, 2010, **36**, 401; b) A.H. El-Sagheer, T. Brown, *Chem. Soc. Rev.*, 2010, **39**, 1388; c) F. Amblard, J. H. Cho, R. F. Schinazi, *Chem. Rev.*, 2009, **109**, 4207.

Unmodified DNA/RNA strands were obtained from commercial suppliers and used without further purification. Fluorescent reference probes were obtained from Exiqon and used after reverse-phase (RP) HPLC purification performed by manufacturer.

Oligonucleotide synthesis was carried out on a PerSpective Biosystems Expedite 8909 instrument in 1 μ mol scale using manufacturer's standard protocols. For incorporation of monomer **M**¹ a hand-coupling procedure was applied (20 min coupling). The coupling efficiencies of standard DNA phosphoramidites and reagent **3** based on the absorbance of the dimethoxytrityl cation released after each coupling varied between 95% and 100%. Cleavage from solid support and removal of nucleobase protecting groups was performed using 32% aqueous ammonia and methylamine 1:1, v/v, for 4 h at rt. The resulting oligonucleotides were purified by DMT-ON RP-HPLC using the Waters System 600 equipped with Xterra MS C18-column (5 μ m, 150 mm \times 7.8 mm). Elution was performed starting with an isocratic hold of A-buffer for 5 min followed by a linear gradient to 70% B-buffer over 40 min at a flow rate of 1.0 mL/min (A-buffer: 0.05 M triethyl ammonium acetate, pH 7.4; B-buffer: 25% buffer A, 75% CH₃CN). RP-purification was followed by detritylation (80% aq. AcOH, 30 min), precipitation (acetone, -18 °C, 12 h) and washing with acetone three times. The identity and purity of oligonucleotides was then verified by MALDI-TOF mass spectrometry and IE HPLC, respectively. IE HPLC was performed using the Merck Hitachi LaChrom instrument equipped with Dionex DNAPac Pa-100 column (250 mm \times 4 mm). Elution was performed starting with an isocratic hold of A- and C-buffers for 2 min followed by a linear gradient to 60% B-buffer over 28 min at a flow rate of 1.0 mL/min (A-buffer: MQ water; B-buffer: 1M NaClO₄, C-buffer: 25mM Tris-Cl, pH 8.0). MALDI-TOF mass-spectrometry analysis was performed using a MALDI-LIFT system on the Ultraflex II TOF/TOF instrument from Bruker and using HPA-matrix (10 mg 3-hydroxypicolinic acid, 50 mM ammonium citrate in 70% aqueous acetonitrile).

Synthesis of monomer **M**¹

Scheme S1^a



^a Reagents and conditions: (i) Pent-4-ynoic acid, HATU, DIPEA, DMF, rt, 1 h, 71%; (ii) NC(CH₂)₂OP(N(*i*-Pr)₂)₂, diisopropylammonium tetrazolide, DCM, rt, 24 h, 73%. DMT = 4,4'-dimethoxytrityl.

(1*R*,3*R*,4*R*,7*S*)-1-(4,4'-Dimethoxytrityloxymethyl)-7-hydroxy-5-(pent-4-ynoyl)-3-(thymine-1-yl)-2-oxa-5-azabicyclo[2.2.1]heptane (2). Pent-4-ynoic acid (287 mg, 2.93 mmol) and HATU (1.11 g, 2.92 mmol) were dissolved in anhydrous DMF (12 mL). DIPEA (0.82 mL, 4.71 mmol) was added and the reaction mixture was stirred at room temperature for 10 min. A solution of nucleoside **1** (1.50 g, 2.62 mmol) in anhydrous DMF (12 mL) was added dropwise, and the reaction mixture was stirred at room temperature for 1 h. The reaction mixture was diluted with ethyl acetate (150 mL) and washed with a saturated aqueous solution of NaHCO₃ (2 × 475 mL) and water (6 × 50 mL). The aqueous phases were back-extracted in portions with ethyl acetate (160 mL in total). The combined organic phase was dried over Na₂SO₄, filtered and the solvent removed *in vacuo*. The residue was purified by silica gel column chromatography (0 – 5% MeOH/CH₂Cl₂) to afford a rotameric mixture (~0.65:0.35 by ¹H NMR) of nucleoside **2** as an off-white foam (1.21 g, 71%). *R*_f 0.57 (10% MeOH/CH₂Cl₂); ¹H NMR (400 MHz, DMSO-*d*₆) (subscript A = major rotamer, subscript B = minor rotamer; integrals are shown only for major rotamer) δ_H 11.46 (s, 1H, NH_A), 11.38 (s, NH_B), 7.56 (s, H6_B), 7.52 (s, H6_A), 7.46 – 7.41 (m, 2H, Ar),

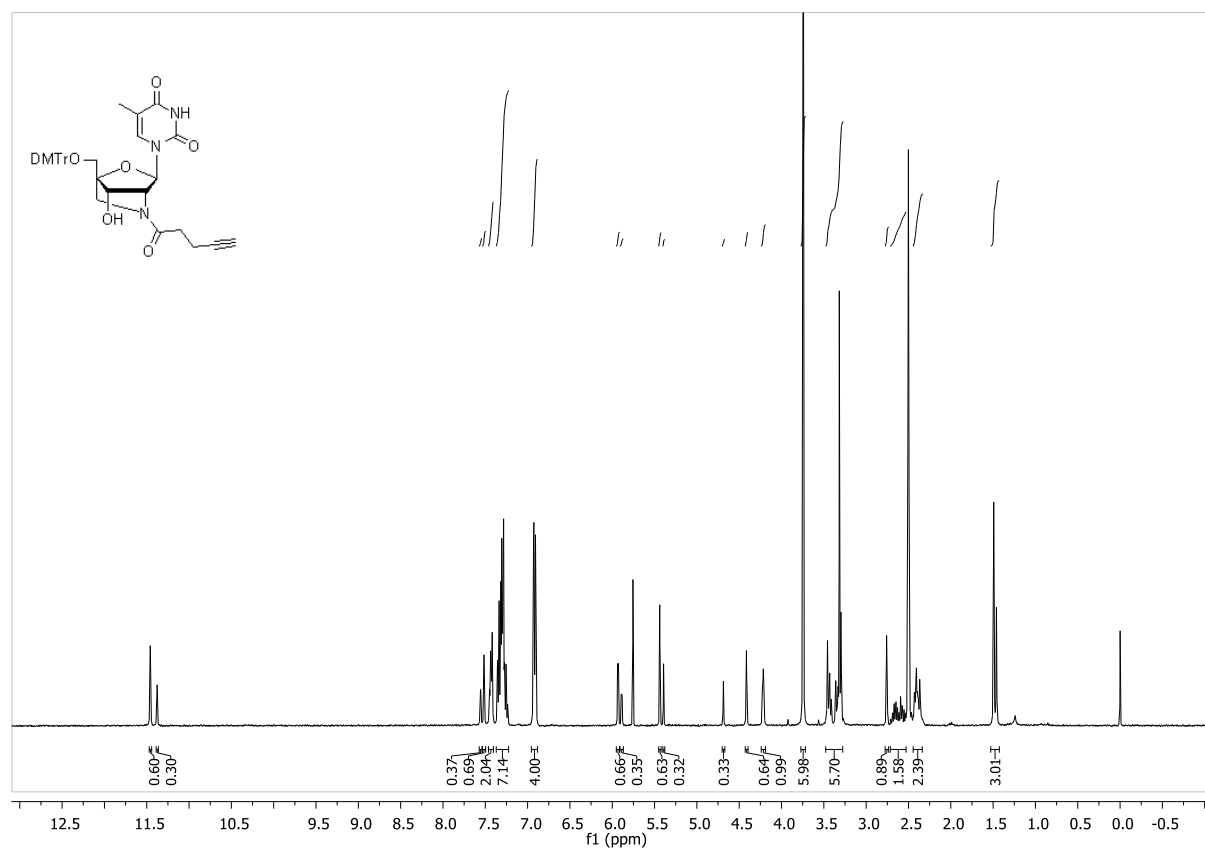
7.37 – 7.22 (m, 7H, Ar), 6.94 - 6.89 (m, 4H, Ar), 5.93 (d, $J = 4.1$ Hz, 1H, 3'-OH_A), 5.89 (d, $J = 4.5$ Hz, 3'-OH_B), 5.44 (s, 1H, H1'_A), 5.39 (s, H1'_B), 4.69 (s, H2'_B), 4.41 (s, 1H, H2'_A), 4.21 (m, 1H, H3'), 3.74 (s, 6H, 2 × OCH₃), 3.47 – 3.28 (m, 4H, H5', H5''), 2.76 (t, $J = 2.3$ Hz, 1H, C≡CH), 2.72 – 2.52, 2.44 – 2.35 (m, 4H, 2 × CH₂), 1.49 (s, 3H, 5-Me_A), 1.46 (s, 1H, 5-Me_B); ¹³C NMR (101 MHz, DMSO-*d*₆) δ_C 169.4, 169.3, 163.9, 163.8, 158.2, 150.0, 149.8, 144.64, 144.58, 135.32, 135.25, 135.04, 135.01, 134.1, 129.8, 129.7, 128.0, 127.7, 126.9, 113.3, 108.6, 108.5, 87.9, 87.3, 86.6, 86.2, 85.8, 85.7, 83.9, 83.8, 71.3, 71.2, 69.2, 68.2, 63.0, 60.7, 59.3, 59.2, 55.1, 51.1, 32.5, 32.0, 13.6, 13.4, 12.29, 12.25; HRMS-ESI *m/z*: 674.2454 ([M + Na]⁺, C₃₇H₃₇N₃O₈-Na⁺ calcd 674.2473).

(1*R*,3*R*,4*R*,7*S*)-7-(2-Cyanoethoxy(diisopropylamino)-phosphinoxy)-1-(4,4'-dimethoxytrityloxymethyl)-5-(pent-4-ynoyl)-3-(thymine-1-yl)-2-oxa-5-azabicyclo[2.2.1]heptane (3).

Nucleoside **2** (176 mg, 0.27 mmol) was co-evaporated with anhydrous CH₂Cl₂, and subsequently mixed with *N,N*-diisopropylammonium tetrazolide (69 mg, 0.40 mmol). The solids were dissolved in anhydrous CH₂Cl₂ (4.0 mL) and 2-cyanoethyl-*N,N,N',N'*-tetraisopropylphosphane (120 μL, 0.38 mmol) was added dropwise. The reaction mixture was stirred at room temperature for 18 h, and then additional *N,N*-diisopropylammonium tetrazolide (49 mg, 0.29 mmol) and 2-cyanoethyl-*N,N,N',N'*-tetraisopropylphosphane (90 μL, 0.28 mmol) were added and stirred for a further 5 h. Ethanol (1 mL) was added and the resulting solution stirred for 20 min. The reaction mixture was then diluted with CH₂Cl₂ (20 mL) and washed with a saturated aqueous solution of NaHCO₃ (2 × 15 mL). The combined aqueous phase was back-extracted with CH₂Cl₂ (3 × 15 mL), and the combined organic phase was dried over Na₂SO₄, filtered and the solvent removed *in vacuo*. The residue was purified by silica gel column chromatography (20–75% ethyl acetate/petroleum ether) giving a white foam. The foam was dissolved in ethyl acetate (1.5 mL) and the resulting solution was added dropwise to petroleum ether (150 mL). The formed precipitate was isolated affording phosphoramidite **3** as a white foam (167 mg, 73%). *R*_f 0.63 (ethyl acetate); ³¹P NMR (162 MHz, DMSO-*d*₆) δ_P 148.3, 147.9, 147.6, 147.0; HRMS-ESI *m/z*: 874.3528 ([M + Na]⁺, C₄₆H₅₄N₅O₉P-Na⁺ calcd 874.3551).

Figure S1. A) ^1H and B) ^{13}C NMR spectra of compound **2** (400 MHz and 101 MHz, $\text{DMSO-}d_6$).

A)



B)

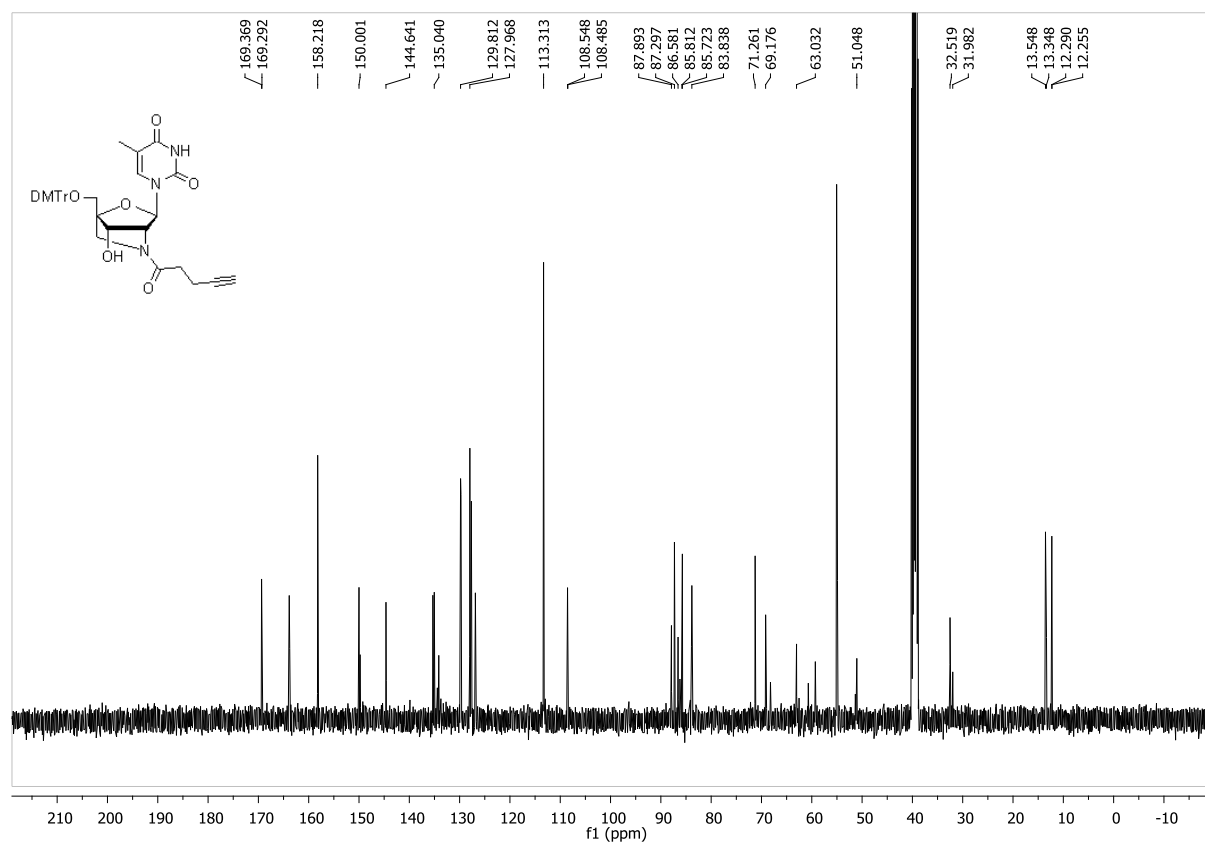
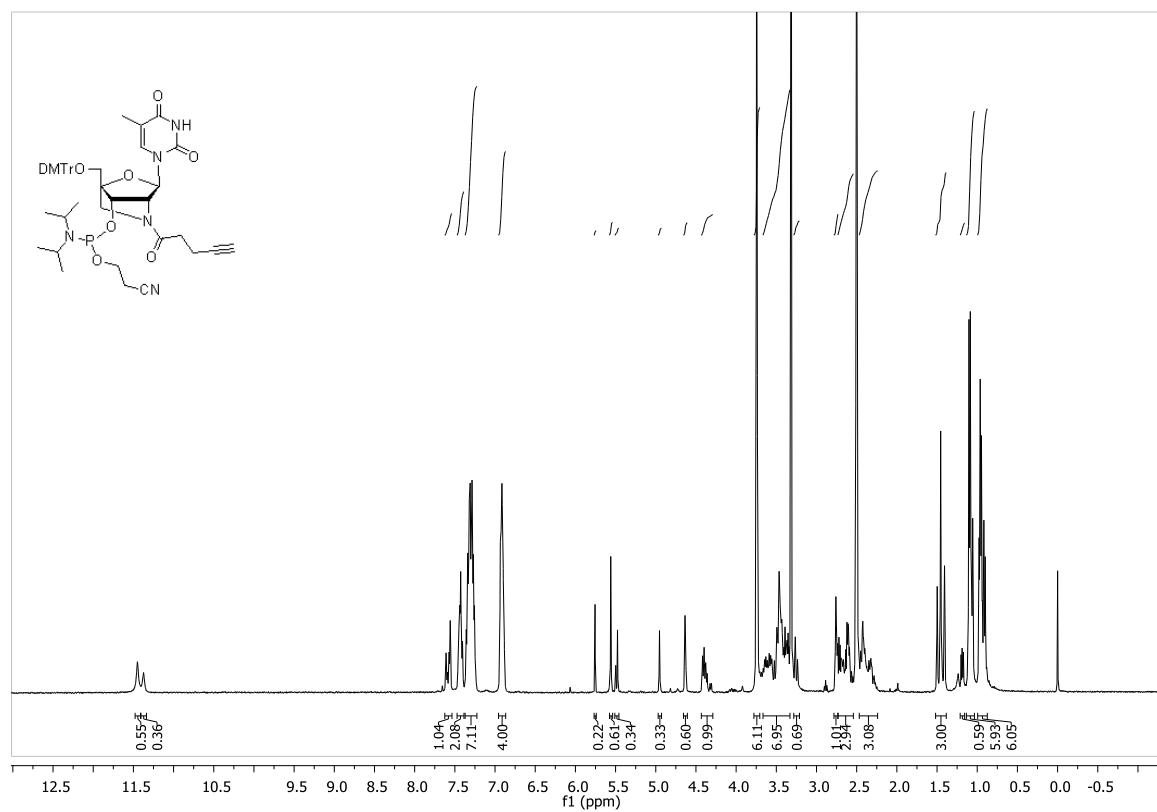


Figure S2. A) ^1H and B) ^{31}P NMR spectra of compound **3** (400 MHz and 162 MHz, $\text{DMSO-}d_6$).

A)



B)

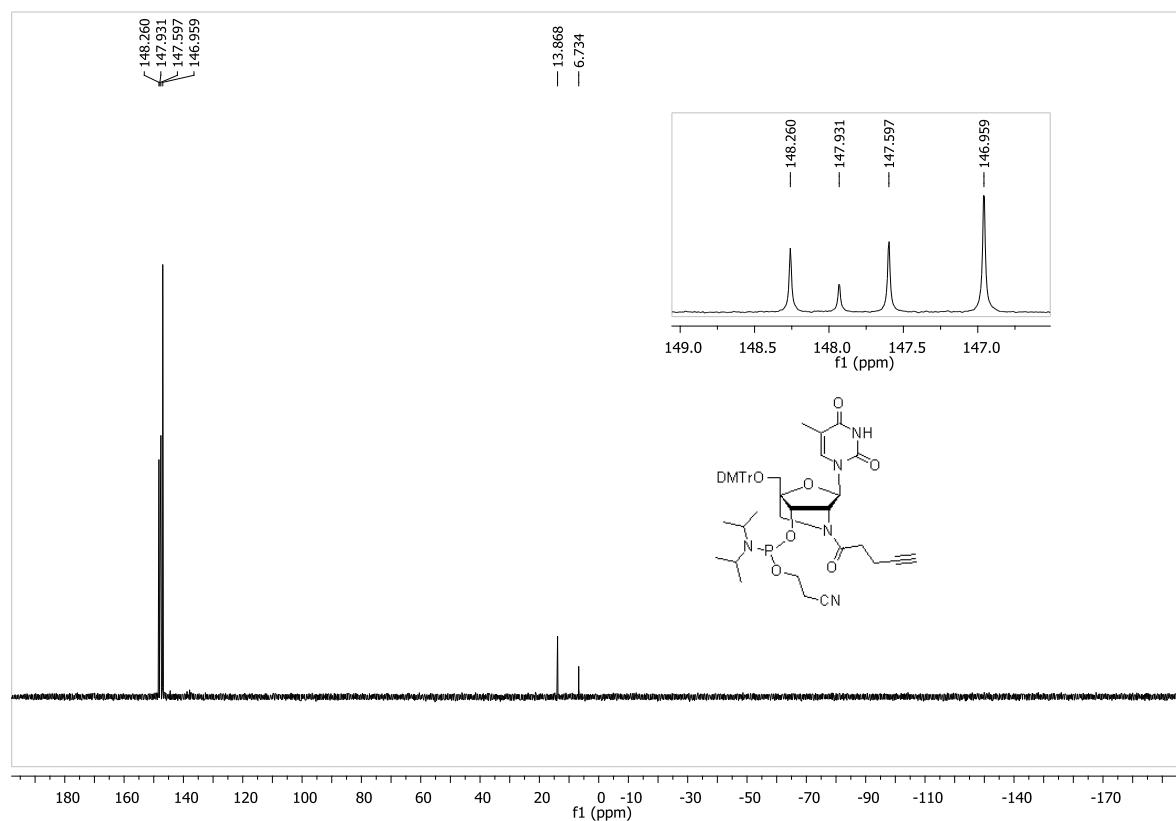
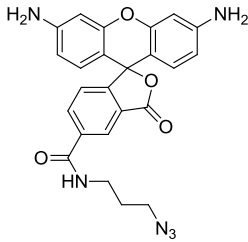
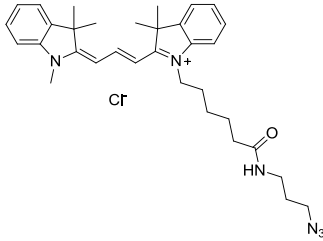
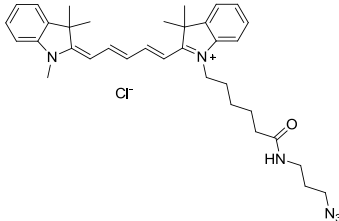
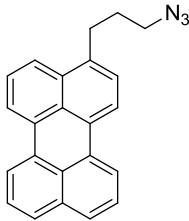
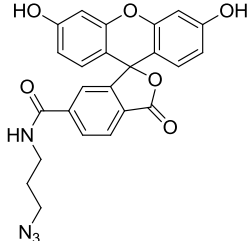
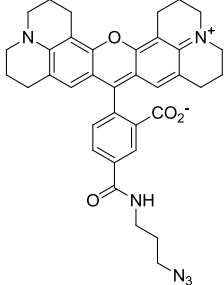


Table S1. Chemical structures and photophysical characteristics of single molecule dyes used in this study.^a

Dye	Chemical structure of azide derivative	λ^{ex} , nm	$\lambda^{\text{fl}}_{\text{max}}$, nm	ϵ_{max} at λ^{ex} , $\text{cm}^{-1}\text{M}^{-1}$	Φ_{F}
5-R110		496	520	80.000	0.9
Cy3		546	563	150.000	0.1
Cy5		646	662	250.000	0.2
Perylene		408, 436	435, 463, 495	28.000, 37.000	0.95
6-FAM		494	520	75.000	0.9
ROX		570	591	82.000	1.0

^a This information is available online, e.g. on web-page of fluorescent dyes supplier Lumiprobe LLC: <http://www.lumiprobe.com/>

Post-synthetic click chemistry

Concentrations of oligonucleotides were calculated using the following extinction coefficients ($\text{OD}_{260}/\mu\text{mol}$): G, 10.5; A, 13.9; T, \mathbf{M}^1 , 7.9; C, 6.6; \mathbf{M}^2 , 11.8; \mathbf{M}^3 , 5.7; \mathbf{M}^4 , 4.3; \mathbf{M}^5 , 33.2.³

General method for CuAAC reactions (monomers \mathbf{M}^2 – \mathbf{M}^4). Starting oligonucleotide **ON1–ON4** (20 nmol) was dissolved in fresh MQ water (30 μL) in 1.5 mL plastic eppendorf tubes. DMSO (40 μL), 2M triethylammonium acetate buffer (pH 7.4; 10 μL), corresponding azide **5–7** (6 μL (**ON1**), 10 μL (**ON2–ON3**) and 14 μL (**ON4**) of 10 mM solution in DMSO), ascorbic acid (5 μL of 25 mM freshly prepared stock solution) and Cu(II)-TBTA equimolar complex (5 μL of 10 mM stock solution) were subsequently added. The resulting mixture was deaerated, tightly closed, mixed by vortexing and left at rt (monomer \mathbf{M}^2 ; 12 h, **ON1–ON3**; 24 h, **ON4**). In case of highly hydrophobic cyanine azides **6–7** the reaction mixture was initially heated to 85 °C for 10 minutes and then left at rt for 12 h (**ON1–ON3**) or 24 h (**ON4**). The reaction was afterwards filtrated through Illustra NAP-10 column (GE Healthcare) following manufacture's protocol. The resulting solution was evaporated followed by precipitation of the product conjugates from cold acetone (-18 °C, 12 h) and subsequent washing with acetone two times. The resulting conjugates **ON5–ON16** were analysed by MALDI TOF mass spectrometry and IE HPLC (Table S2, Figures S3-S4). Final yields of products based on the absorbance at 260 nm: 85% (**ON5**), 78% (**ON6**), 80% (**ON7**), 74% (**ON8**), 63% (**ON9**), 63% (**ON10**), 63% (**ON11**), 62% (**ON12**), 64% (**ON13**), 58% (**ON14**), 60% (**ON15**), 67% (**ON16**).

General method for microwave-assisted CuAAC reactions (monomer \mathbf{M}^5). Starting oligonucleotide **ON1–ON4** (20 nmol) was dissolved in fresh MQ water (30 μL) in 1.5 mL plastic eppendorf tubes. DMSO (40 μL), 2M triethylammonium acetate buffer (pH 7.4; 10 μL), corresponding azide **8** (6 μL (**ON1**), 10 μL (**ON2–ON3**) and 14 μL (**ON4**) of 10 mM solution in DMSO), ascorbic acid (5 μL of 25

³ I. K. Astakhova, J. Wengel, *Chem. Eur. J.* 2013, 1112-1122.

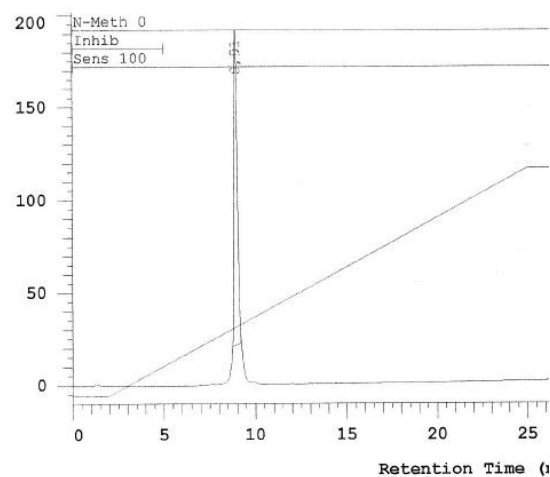
mM freshly prepared stock solution) and Cu(II)-TBTA equimolar complex (5 μ L of 10 mM stock solution) were subsequently added. The resulting mixture was deaerated, tightly closed, mixed by vortexing and subjected to microwave conditions (microwave reactor, 60 °C, 15 minutes). The reaction was afterwards cooled to room temperature and filtrated through Illustra NAP-10 column (GE Healthcare) following manufacture's protocol. The resulting solution was evaporated followed by precipitation of the product conjugates from cold acetone (-18 °C, 12 h) and subsequent washing with acetone two times. The resulting conjugates **ON17–ON20** were analysed by MALDI TOF mass spectrometry and IE HPLC (Table S2, Figures S3-S4). Final yields of products based on the absorbance at 260 nm: 81% (**ON17**), 72% (**ON18**), 76% (**ON19**), 65% (**ON20**).

Table S2. IE HPLC retention times and MALDI MS of purified oligodeoxyribonucleotides.

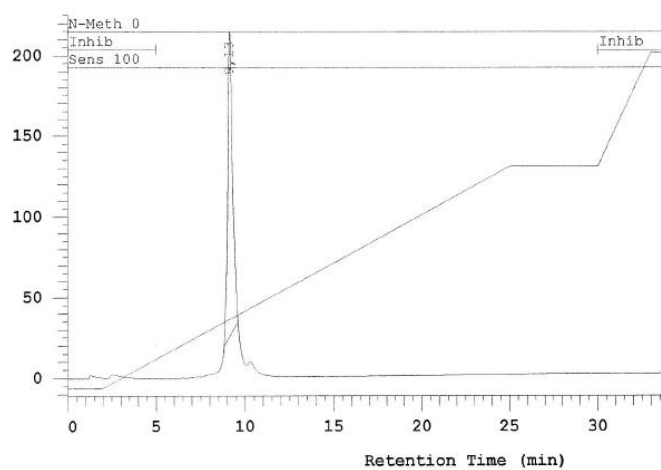
#	Sequence, 5'→3'	Ret. time, min	MALDI MS	
			Found m/z [M+H] ⁺	Calc. m/z [M+H] ⁺
ON1	TGC ACT CTA TGM ¹ CTG TAT CAT	8.88	6467	6468
ON2	TGC ACT CTA M ¹ GT CM ¹ G TAT CAT	8.91	6575	6575
ON3	TGC ACM ¹ CTA TGT CTG TAM ¹ CAT	8.90	6572	6575
ON4	TGC ACM ¹ CTA TGM ¹ CTG TAM ¹ CAT	8.91	6680	6682
ON5	TGC ACT CTA TGM ² CTG TAT CAT	9.10	6925	6925
ON6	TGC ACT CTA M ² GT CM ² G TAT CAT	9.13	7491	7488
ON7	TGC ACM ² CTA TGT CTG TAM ² CAT	9.13	7489	7488
ON8	TGC ACM ² CTA TGM ² CTG TAM ² CAT	9.34	8053	8052
ON9	TGC ACT CTA TGM ³ CTG TAT CAT	10.00	7008	7008
ON10	TGC ACT CTA M ³ GT CM ³ G TAT CAT	10.01	7657	7655
ON11	TGC ACM ³ CTA TGT CTG TAM ³ CAT	10.20	7655	7655
ON12	TGC ACM ³ CTA TGM ³ CTG TAM ³ CAT	10.42	8300	8302
ON13	TGC ACT CTA TGM ⁴ CTG TAT CAT	11.40	7031	7034
ON14	TGC ACT CTA M ⁴ GT CM ⁴ G TAT CAT	11.45	7707	7707
ON15	TGC ACM ⁴ CTA TGT CTG TAM ⁴ CAT	11.50	7706	7707
ON16	TGC ACM ⁴ CTA TGM ⁴ CTG TAM ⁴ CAT	11.93	8381	8379
ON17	TGC ACT CTA TGM ⁵ CTG TAT CAT	9.11	6800	6803
ON18	TGC ACT CTA M ⁵ GT CM ⁵ G TAT CAT	9.11	7242	7245
ON19	TGC ACM ⁵ CTA TGT CTG TAM ⁵ CAT	9.20	7244	7245
ON20	TGC ACM ⁵ CTA TGM ⁵ CTG TAM ⁵ CAT	9.39	7688	7687

Figure S3. Representative IE HPLC of modified oligonucleotides.

ON2



ON6



ON10

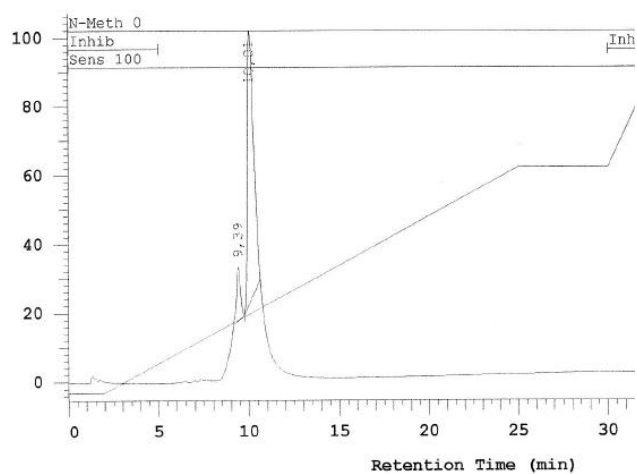
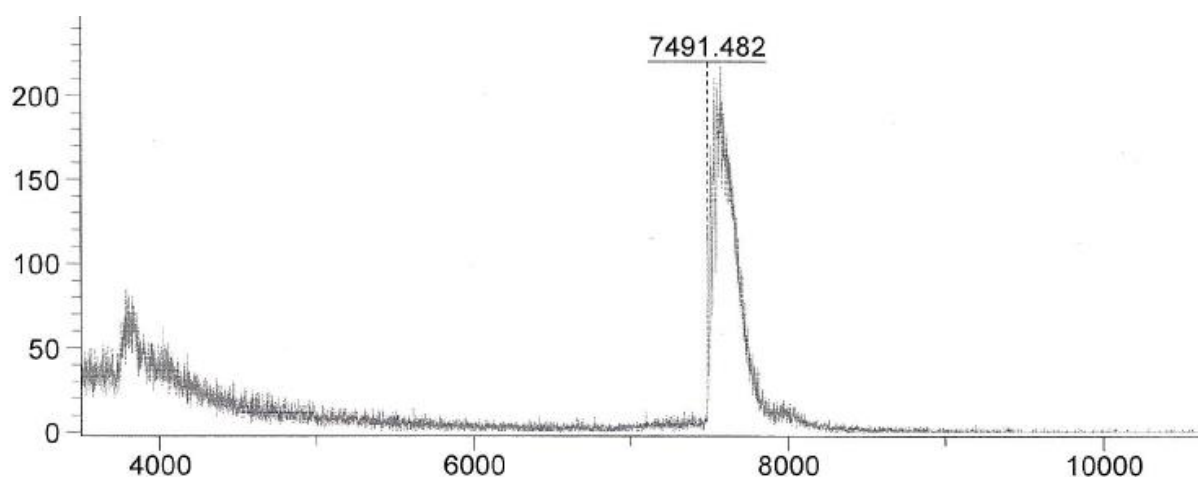


Figure S4. Representative MALDI-MS spectra of modified oligonucleotide ON6.



UV-visible absorbance and thermal denaturation studies

UV-visible absorbance spectra and thermal denaturation experiments were performed on a Beckman Coulter DU800 UV/VIS Spectrophotometer equipped with Beckman Coulter High Performance Temperature Controller in a medium salt phosphate buffer (100 mM NaCl, 10 mM Na-phosphate, 0.1 mM EDTA, pH 7.0). Concentrations of oligonucleotides were calculated using the extinction coefficients listed above. Annealing steps were performed on Eppendorf Thermomixer Shaker equipped with a 0.5 mL block. Oligonucleotides (1.0 μ M each strand) were thoroughly mixed, denaturated by heating for 5 min at 85 $^{\circ}$ C and subsequently cooled to the starting temperature of experiment. Thermal denaturation temperatures (T_m values, $^{\circ}$ C) were determined as the maximum of the first derivative of the thermal denaturation curve (A vs. temperature). Reported T_m values are an average of at least two measurements within ± 0.5 $^{\circ}$ C.

Table S3. T_m values of the modified duplexes containing monomers M^2-M^5 compared to corresponding M^1 -labelled references.^a

ON#	Sequence, 5'→3'	$\Delta T_m, ^\circ C^*$	
		DNA	RNA
ON5	TGC ACT CTA TGM ² CTG TAT CAT	-3.0	-3.0
ON6	TGC ACT CTA M ² GT CM ² G TAT CAT	-3.5	-3.0
ON7	TGC ACM ² CTA TGT CTG TAM ² CAT	-5.5	-4.0
ON8	TGC ACM ² CTA TGM ² CTG TAM ² CAT	-7.0	-5.0
ON9	TGC ACT CTA TGM ³ CTG TAT CAT	0.0	-2.0
ON10	TGC ACT CTA M ³ GT CM ³ G TAT CAT	-0.5	-3.0
ON11	TGC ACM ³ CTA TGT CTG TAM ³ CAT	0.0	-3.0
ON12	TGC ACM ³ CTA TGM ³ CTG TAM ³ CAT	0.0	-4.5
ON13	TGC ACT CTA TGM ⁴ CTG TAT CAT	0.0	-2.0
ON14	TGC ACT CTA M ⁴ GT CM ⁴ G TAT CAT	+1.5	-4.0
ON15	TGC ACM ⁴ CTA TGT CTG TAM ⁴ CAT	0.0	-3.5
ON16	TGC ACM ⁴ CTA TGM ⁴ CTG TAM ⁴ CAT	0.0	-5.5
ON17	TGC ACT CTA TGM ⁵ CTG TAT CAT	+4.0	0.0
ON18	TGC ACT CTA M ⁵ GT CM ⁵ G TAT CAT	+6.5	-9.0
ON19	TGC ACM ⁵ CTA TGT CTG TAM ⁵ CAT	+4.0	-1.0
ON20	TGC ACM ⁵ CTA TGM ⁵ CTG TAM ⁵ CAT	+7.0	-1.0

^a Thermal denaturation temperatures in a medium salt phosphate buffer T_m ($^\circ C$) measured as the maximum of the first derivatives of the melting curves (A vs temperature). Reported T_m values are averages of at least two measurements with resulting $T_m \pm 0.5$ $^\circ C$. * $\Delta T_m = T_m$ (duplex containing monomer M^2-M^5) - T_m (corresponding M^1 -labelled reference).

Table S4. Effect of single-nucleotide mismatch on binding affinity and fluorescence sensing of DNA/RNA targets by **ON7** and **ON19** in a medium salt buffer.^a

Probe: Target DNA/RNA ^a	$T_m/^{\circ}\text{C}$								
	$(I^0/I)^*$								
	DNA target					RNA target			
	X	A	C	T	G	A	C	U	G
Probe ON7									
5' - TGC ACM ² CTA TGT CTG TAM ² CAT		47.0	46.0	44.0	58.0 ^{cc}	50.0	51.0	54.0	64.0 ^{cc}
3' - ACG TGA GAT ACA GAC ATA XTA		(4.4)	(4.1)	(3.4)		(6.3)	(4.0)	(3.7)	
5' - TGC ACM ² CTA TGT CTG TAM ² CAT		58.0 ^{cc}	50.0	48.5	45.0	64.0 ^{cc}	55.0	51.0	56.0
3' - ACG TGA GAT ACA GAC ATX GTA			(1.9)	(2.1)	(3.5)		(2.3)	(2.0)	(4.4)
5' - TGC ACM ² CTA TGT CTG TAM ² CAT		58.0 ^{cc}	45.0	n.t.	47.0	64.0 ^{cc}	51.0	52.5	54.0
3' - ACG TGA GAT ACX GAC ATA GTA			(3.4)	(4.3)	(5.5)		(3.5)	(3.6)	(5.8)
Probe ON19									
5' - TGC ACM ⁵ CTA TGT CTG TAM ⁵ CAT		63.0	59.5	55.0	67.0 ^{cc}	60.0	58.0	55.0	67.0 ^{cc}
3' - ACG TGA GAT ACA GAC ATA XTA		(5.6)	(5.5)	(3.9)		(8.1)	(5.8)	(5.2)	
5' - TGC ACM ⁵ CTA TGT CTG TAM ⁵ CAT		67.0 ^{cc}	56.0	52.0	54.0	67.0 ^{cc}	53.0	52.5	49.0
3' - ACG TGA GAT ACA GAC ATX GTA			(4.5)	(6.2)	(9.1)		(5.6)	(7.8)	(9.9)
5' - TGC ACM ⁵ CTA TGT CTG TAM ⁵ CAT		67.0 ^{cc}	55.0	52.0	52.5	67.0 ^{cc}	53.0	n.t.	54.0
3' - ACG TGA GAT ACX GAC ATA GTA			(5.2)	(4.5)	(6.0)		(4.8)	(5.0)	(7.9)

^a Sequences of DNA target variants are displayed; cc = complementary complex; n. t. = no clear transition detected. T_m values measured using 0.5 μM concentration of complementary strands.

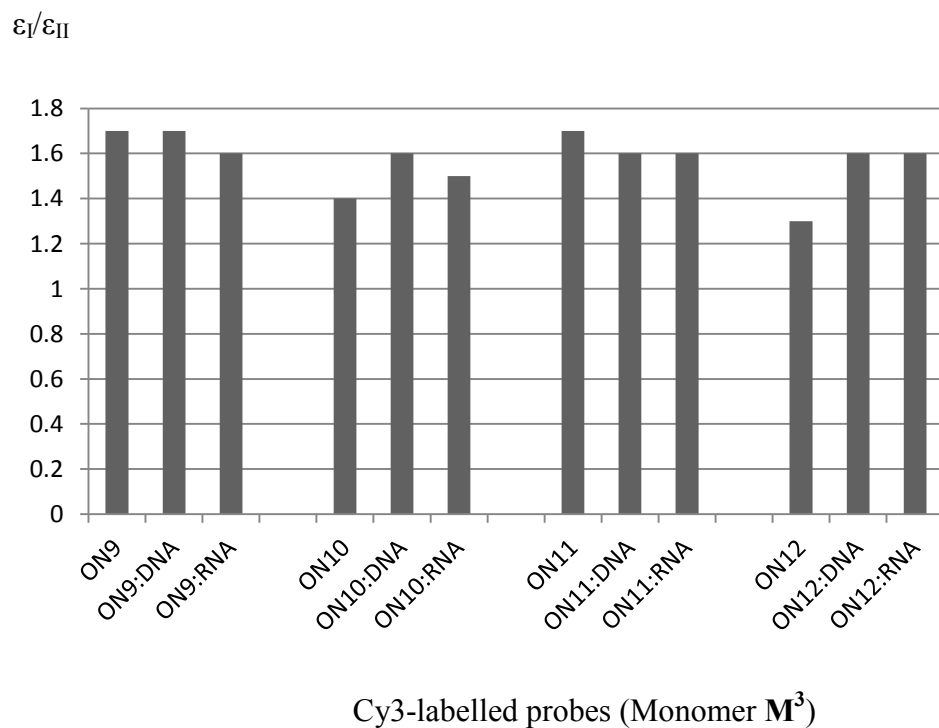
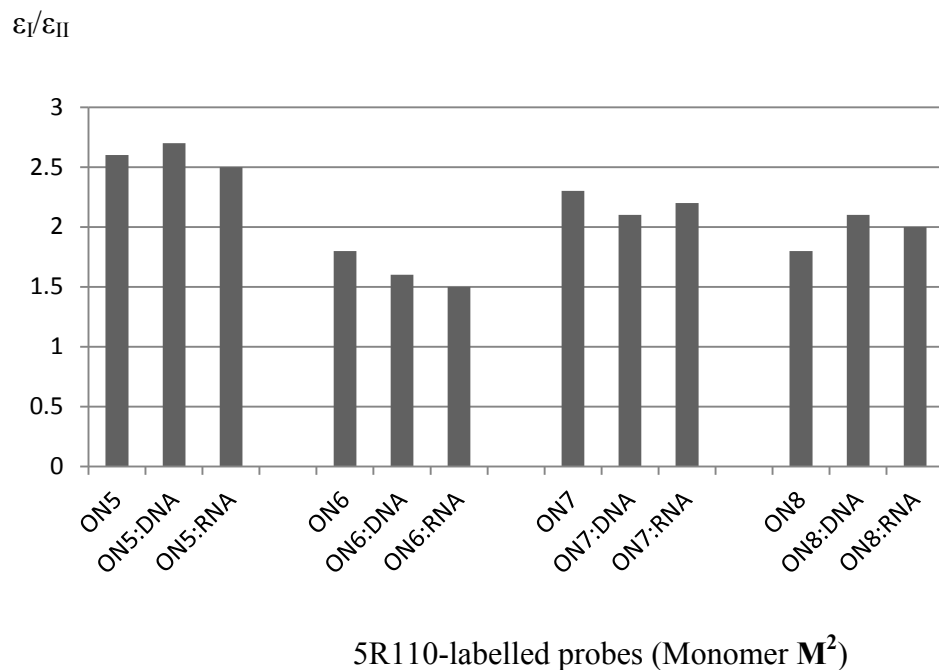
* I^0/I = a ratio of fluorescence intensity of fully complementary to mismatched complex, respectively. Fluorescence intensity values were obtained as described below using 1.0 μM LNA/DNA probes, excitation wavelengths of 500 nm (**ON7**) and 425 nm (**ON19**), and monitoring emission at 530 nm and 458 nm, respectively.

Table S5. T_m values of the modified duplexes containing monomers M^2 – M^5 measured at the fluorophores' absorbance wavelength.^a

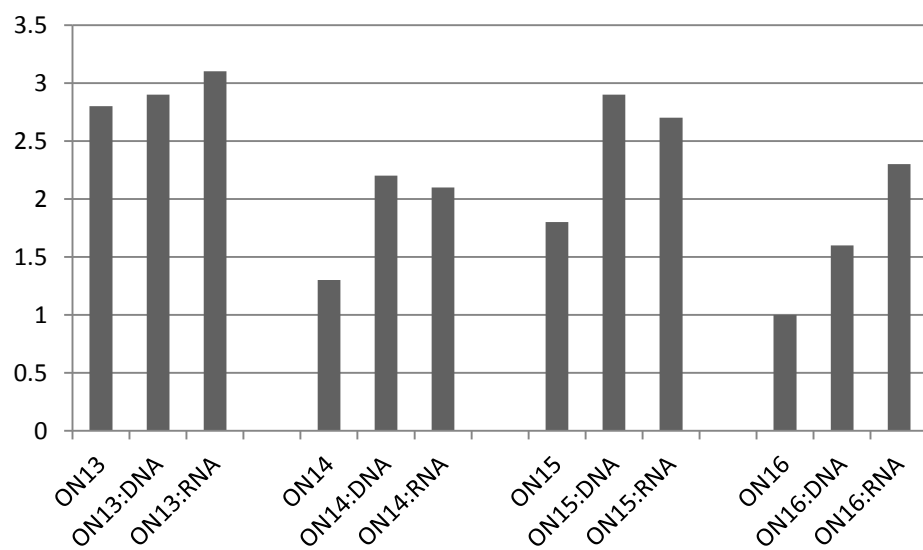
ON#	Sequence, 5'→3'	T_m , °C	
		DNA	RNA
ON5	TGC ACT CTA TGM ² CTG TAT CAT	58.5	62.0
ON6	TGC ACT CTA M ² GT CM ² G TAT CAT	60.0	66.0
ON7	TGC ACM ² CTA TGT CTG TAM ² CAT	59.0	64.0
ON8	TGC ACM ² CTA TGM ² CTG TAM ² CAT	57.0	65.0
ON9	TGC ACT CTA TGM ³ CTG TAT CAT	62.0	63.0
ON10	TGC ACT CTA M ³ GT CM ³ G TAT CAT	63.0	65.5
ON11	TGC ACM ³ CTA TGT CTG TAM ³ CAT	62.0	65.0
ON12	TGC ACM ³ CTA TGM ³ CTG TAM ³ CAT	65.0	65.0
ON13	TGC ACT CTA TGM ⁴ CTG TAT CAT	62.0	63.0
ON14	TGC ACT CTA M ⁴ GT CM ⁴ G TAT CAT	63.0	64.0
ON15	TGC ACM ⁴ CTA TGT CTG TAM ⁴ CAT	63.0	64.0
ON16	TGC ACM ⁴ CTA TGM ⁴ CTG TAM ⁴ CAT	65.0	64.5
ON17	TGC ACT CTA TGM ⁵ CTG TAT CAT	65.5	65.0
ON18	TGC ACT CTA M ⁵ GT CM ⁵ G TAT CAT	n.t.*	n.t.
ON19	TGC ACM ⁵ CTA TGT CTG TAM ⁵ CAT	67.0	n. t.
ON20	TGC ACM ⁵ CTA TGM ⁵ CTG TAM ⁵ CAT	72.0	70.0

^a Thermal denaturation temperatures in a medium salt phosphate buffer T_m (°C) measured as the maximum of the first derivatives of the melting curves (A vs temperature). The fluorophore's absorbance wavelength used in this study: M^2 , 503 nm; M^3 , 548 nm; M^4 , 645 nm; M^5 , 450 nm. Reported T_m values are averages of at least two measurements with resulting $T_m \pm 0.5$ °C. * n.t. = no transition detected.

Figure S5. Ratio I/II of absorbance maxima of modified oligonucleotides and duplexes.

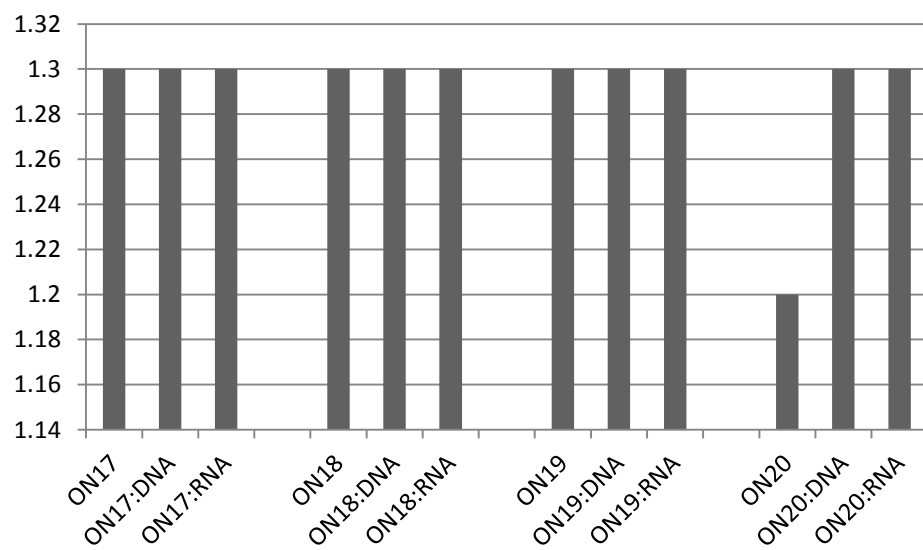


ϵ_I/ϵ_{II}



Cy5-labelled probes (Monomer M^4)

ϵ_I/ϵ_{II}



Perylene-labelled probes (Monomer M^5)

Fluorescence studies

Fluorescence spectra were obtained in the medium salt buffer using a PerkinElmer LS 55 luminescence spectrometer equipped with a Peltier Temperature Programmer. For recording of fluorescence spectra, an excitation wavelength of 500 nm (**M**²), 545 nm (**M**³), 645 nm (**M**⁴), 425 nm (**M**⁵), and 0.25–1.0 μM concentrations of the oligonucleotides were used.

Quantum yields Φ_F were determined by a relative method following described procedure.⁴ Quantum yields of fluorescent probes containing monomers **M**² and **M**⁵ were determined using highly diluted solutions of 9,10-diphenylanthracene and perylene in cyclohexane. Quantum yields of fluorescent probes containing monomers **M**³–**M**⁴ were determined using highly diluted solutions of crezyl violet perchlorate and oxazine 170 in ethanol and methanol, respectively. Selected excitation wavelengths for quantum yield measurements: 480 nm (**M**²), 515 nm (**M**³), 600 nm (**M**⁴), 425 nm (**M**⁵) which correspond to excitation maxima of the probes (data not shown).

Fluorescence brightness (FB) values were calculated using equation:

$$FB = \epsilon_{\max} \times \Phi_F,$$

Where ϵ_{\max} is the maximal molar extinction coefficient of the probe and Φ_F is the corresponding fluorescence quantum yield.

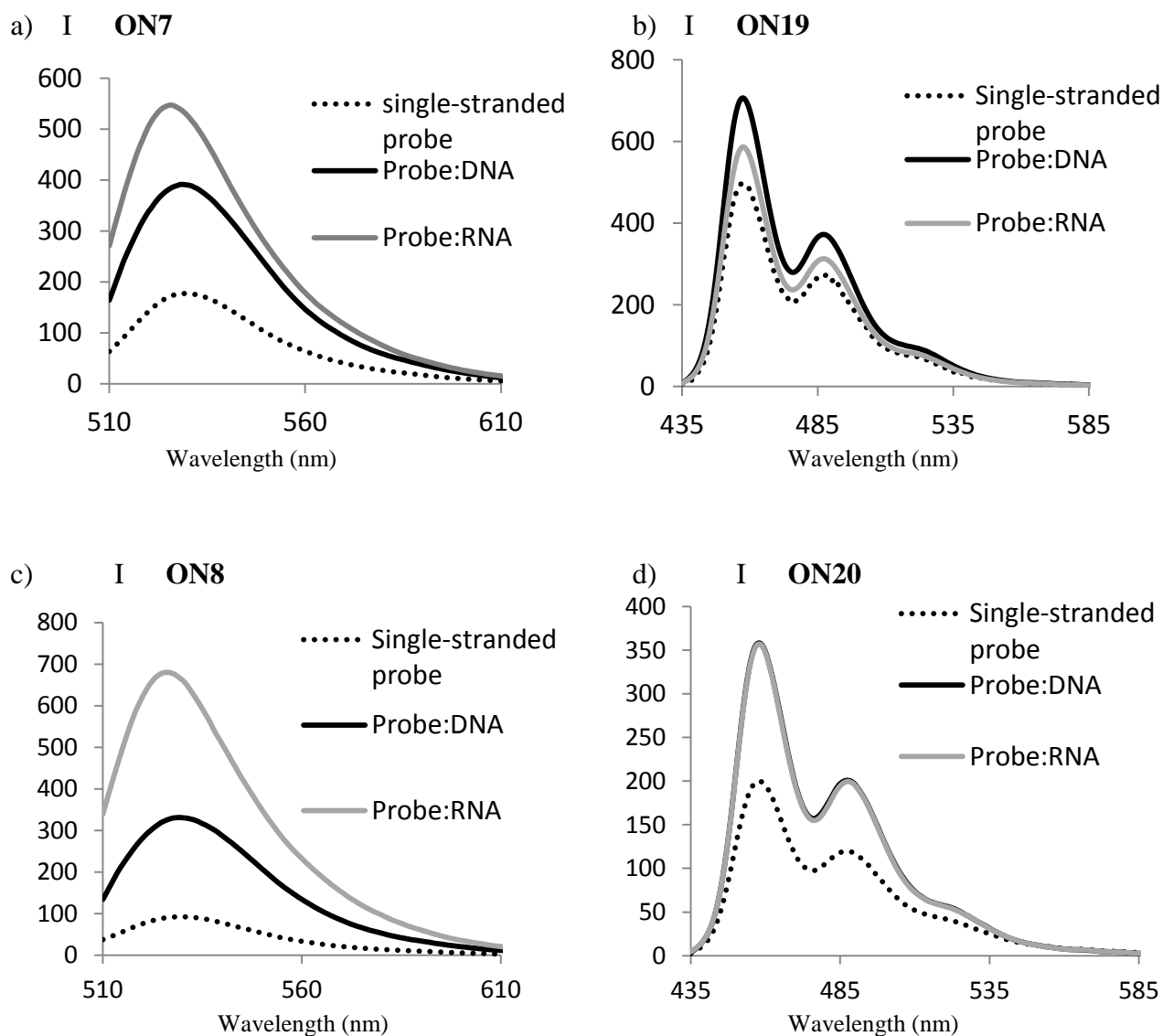
⁴ J. R. Lakowicz, *Principles of Fluorescence Spectroscopy*, 3th. Ed., Springer, Singapore, **2006**.

⁵ D. Lindegaard, A. S. Madsen, I. V. Astakhova, A. D. Malakhov, B. R. Babu, V. A. Korshun, J. Wengel, *Bioorg. Med. Chem.*, 2008, **16**, 94.

Table S6. Spectroscopic and photophysical properties of modified single-stranded probes (SSP) and duplexes.

#	$\lambda_{\text{max}}^{\text{abs}}$, bands I, II (nm)			$\lambda_{\text{max}}^{\text{fl}}$ (nm)			Φ_{F}			FB		
	Duplex with			Duplex with			Duplex with			Duplex with		
	SSP	complementary		SSP	complementary		SSP	complementary		SSP	complementary	
		DNA	RNA		DNA	RNA		DNA	RNA		DNA	RNA
ON5	510, 475	503, 473	503, 473	528	525	525	0.21	0.33	0.42	14	24	30
ON6	511, 480	503, 478	503, 478	526	525	525	0.16	0.20	0.25	19	23	29
ON7	510, 480	507, 476	504, 480	530	530	526	0.15	0.42	0.45	20	50	56
ON8	513, 480	507, 474	504, 477	530	529	527	0.05	0.22	0.41	8	39	77
ON9	550, 517	548, 516	547, 516	562	562	560	0.10	0.11	0.10	22	23	12
ON10	550, 517	548, 516	548, 516	563	560	560	0.06	0.10	0.05	11	22	11
ON11	550, 516	548, 516	548, 516	562	560	560	0.05	0.04	0.04	9	9	9
ON12	550, 514	549, 515	546, 515	565	561	558	0.01	0.02	0.01	2	5	3
ON13	647, 603	650, 605	643, 600	662	661	658	0.01	0.01	0.01	2	2	2
ON14	646, 600	646, 601	644, 601	660	659	660	0.01	0.01	0.01	3	3	3
ON15	646, 600	646, 601	645, 601	659	659	659	0.01	0.01	0.01	1	2	2
ON16	646, 599	646, 599	644, 599	659	659	659	0.01	0.01	0.01	1	2	3
ON17	451, 424	452, 426	452, 426	487,457	487,458	487,458	0.89	1.00	1.00	22	26	24
ON18	451, 424	452, 424	452, 424	487,456	488,458	488,458	0.95	1.00	1.00	50	60	56
ON19	451, 424	451, 424	451, 424	489,457	489,457	489,457	0.84	1.00	1.00	49	69	58
ON20	452, 424	454, 424	452, 454	488,459	487,458	487,458	0.54	0.91	0.91	41	80	71

Figure S6. Representative fluorescence spectra of the modified oligonucleotides and duplexes.



Steady-state fluorescence emission spectra of single-stranded probes **ON7** (A), **ON19** (B), **ON8** (C) and **ON20** (D) and their duplexes with complementary DNA/RNA. Spectra were obtained in a medium salt buffer at 19 °C using $\lambda^{\text{ex}} = 500$ nm (A, C), 425 nm (B, D), and 1.0 μM concentrations of oligonucleotides.

* For the duplexes of **ON20** with complementary DNA/RNA the curves are superimposed.

Autoantibody binding assay

General

The human monoclonal autoantibodies were purchased from Diarect AG (dsDNA-mAb32 and dsDNA-mAb33 correspond to clones 32.B9 and 33. H11, respectively).⁶ BSA, human IgG1 kappa and human IgG3 kappa used as reference proteins⁷ were obtained from Sigma-Aldrich and dissolved in a medium salt phosphate buffer (pH 7.4) at concentrations 1.0 mg/mL.

Incubation and Analysis

To a solution of corresponding nucleic acid complex prepared as described above in a plastic 1.5 mL tube (500 μ L 0.5 μ M), 0.5×10^5 IU of the target autoantibody was added (53 μ L, dsDNA-mAb32 9.4×10^5 IU/mL at a protein concentration 0.43 mg/mL; 128 μ L, dsDNA-mAb33 3.9×10^5 IU/mL at a protein concentration 0.70 mg/mL).⁸ As a reference, 50 μ L of the BSA, IgG1 or IgG3 stock solution was used in similar incubation reactions with the probes. Incubation was performed on Eppendorf Thermomixer Shaker (400 rpm) at 37 °C for 3 h. Upon cooling to ambient temperature over 4 h, the resulting solutions were analysed by fluorescence spectroscopy using excitation wavelength 500 nm and monitoring fluorescence at 530 nm.

Limit of target detection (LOD) values were determined by series of incubations and subsequent analysis of dsDNA-mAb33 at concentrations ($\times 10^5$): 1 IU/mL, 0.5 IU/mL, 0.25 IU/mL, 0.1 IU/mL, 0.05 IU/mL, 0.01 IU/mL, and ON7:DNA at concentration 0.5 μ M as described above. Fluorescence intensities were measured at $\lambda^{fl} = 530$ nm. Resulting target titration curve revealed $LOD < 2.5 \times 10^3$ IU/mL, corresponding to the autoantibody concentration < 4.6 μ g/mL (Figure S7).

⁶ T. H. Winkler, S. Jahn, J. R. Kalden, *Clin. Exp. Immunol.*, 1991, **21**, 1019.

⁷ Y. Zhanga, X. Sun, *Chem. Commun.* 2011, **47**, 3927.

⁸ Concentrations of the autoantibodies were determined by ELISA. Chosen concentrations correspond to averaged of the total serum protein (K. D. Pagana, T. J. Pagana 2010, *Mosby's Manual of Diagnostic and Laboratory Tests*, 4th ed. St. Louis: Mosby Elsevier). Other literature consulted for the performed study: a) C. C. Chernecky, B. J. Berger, *Laboratory Tests and Diagnostic Procedures*, 2008, 5th ed. St. Louis: Saunders; b) *Handbook of Diagnostic Tests*, 2003, 3rd ed. Philadelphia: Lippincott Williams and Wilkins.

Table S7. Fluorescence detection of antibody binding by single-stranded oligonucleotides and duplexes containing monomer M².

Target	Probe:	Fluorescence intensity at 530 nm					
		ssON7	ON7: DNA	ON7: RNA	ssON8	ON8: DNA	ON8: RNA
-		83	122	148	35	73	176
dsDNA-mAb32	<i>0*</i>						
		34	166	208	19	129	249
dsDNA-mAb33	<i>0*</i>						
		71	690	242	36	120	291
BSA	<i>0*</i>						
		98	171	256	26	110	218
IgG1	<i>0*</i>						
		90	120	132	21	84	165
IgG3	<i>0*</i>						
		100	110	120	20	65	153

* No fluorescence signal observed for proteins at λ^{fl} 530 nm.

Molecular modeling of the interactions between fluorescent probes and proteins used in this study

Duplexes were built in A/B-type helical geometry using Chem3D Pro 12.0 for incorporation of fluorophores and further analysed by MacroModel V9.1.⁹ When doing this the structures were minimized using the Polak–Ribiere conjugate gradient method, the all-atom AMBER force field¹⁰, and GB/SA solvation model¹¹ as implemented in MacroModel V9.1. Non-bonded interactions were treated with extended cut-offs (van der Waals 8.0 Å and electrostatics 20.0 Å). Interaction of the minimized duplex structures with target proteins were studied using Swiss-Pdb Viewer 4.1.0. Structures of the autoantibodies and BSA were imported from Pdb bank and used in building of models without modification.¹² The modeling of protein–nucleic acid interactions was performed assuming 1:1 Langmuir autoantibody–DNA binding model implied recently by surface plasmon resonance (SPR) studies.¹³ Resulting structures were additionally illustrated in PyMOL Molecular Graphics System.

⁹ MacroModel, version 9.1, Schrödinger, 2005, LLC, New York, NY.

¹⁰ S. J. Weiner, P. A. Kollman, D. A. Case, U. C. Singh, C. Ghio, G. Alagona, S. Profeta, P. J. Weiner, *J. Am. Chem. Soc.*, 1984, **106**, 765.

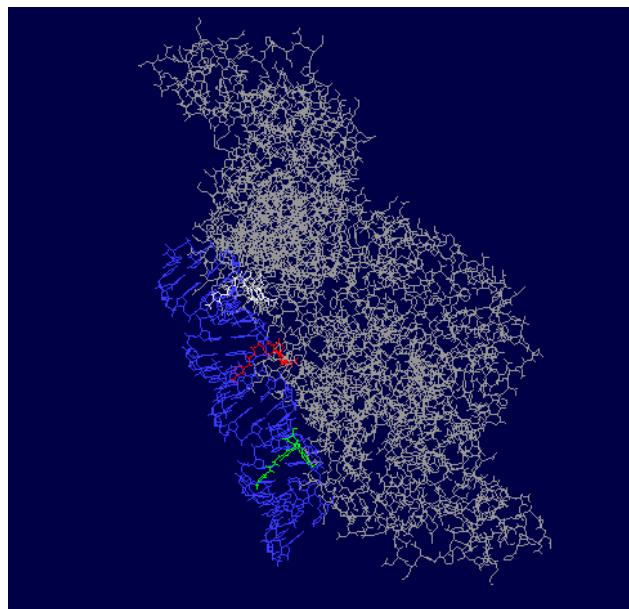
¹¹ S. J. Weiner, P. A. Kollman, D. T. Nguen, D. A. Case, *J. Comput. Chem.*, 1986, **7**, 230.

¹² 64M-2 antibody Fab fragment (used in Figure S8 A,C): H. Yokoyama et. al., *Acta Crystallogr., Sect.D*, 2012, **68**, 232. ED-10 Autoantibody: S. Sanguineti et al., *J. Mol. Biol.* 2007, **370**, 183 (Figure S8 B). BSA: A. Bujacz, G. Bujacz, *Acta Crystallogr.,Sect.D*, 2012, **68**, 1278 (Figure S8 D).

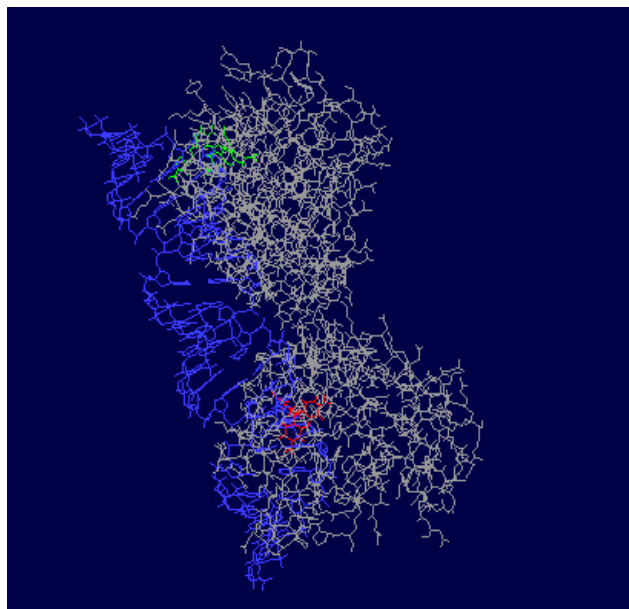
¹³ A. Buhl et al., *Biosens. Bioelectron.*, 2009, **25**, 198.

Figure S7. Molecular modeling of interactions between fluorescent nucleic acid complexes and proteins used in this study.

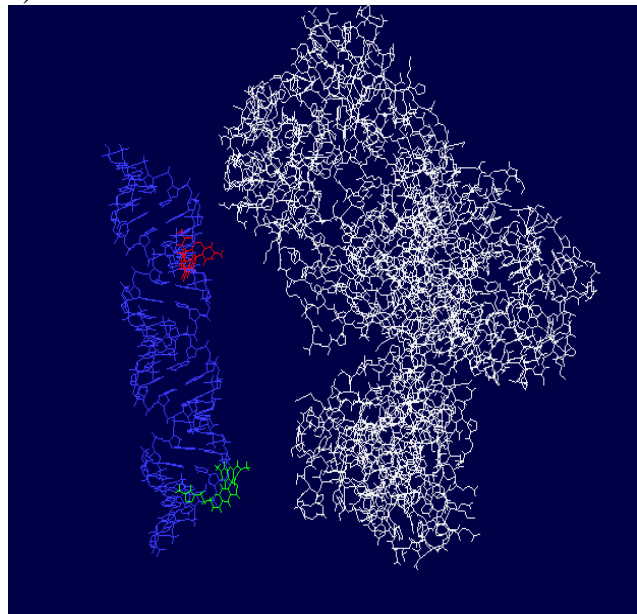
a) **ON8:DNA – BSA**



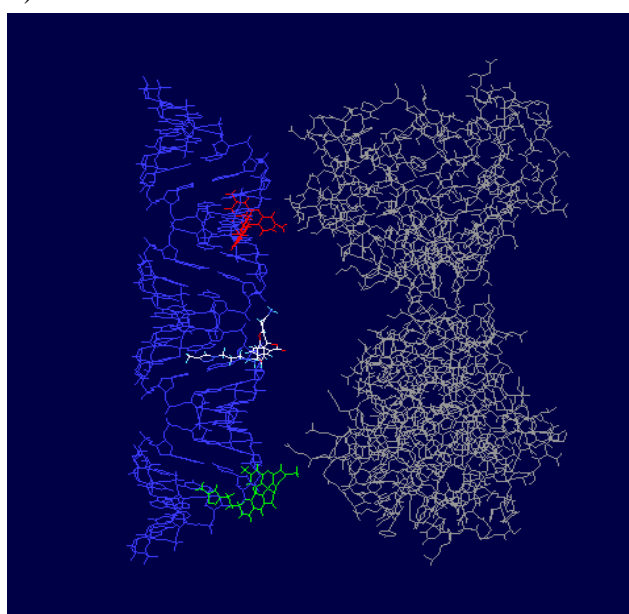
b) **ON7:DNA – mAb33**



c) **ON7:DNA – mAb32**

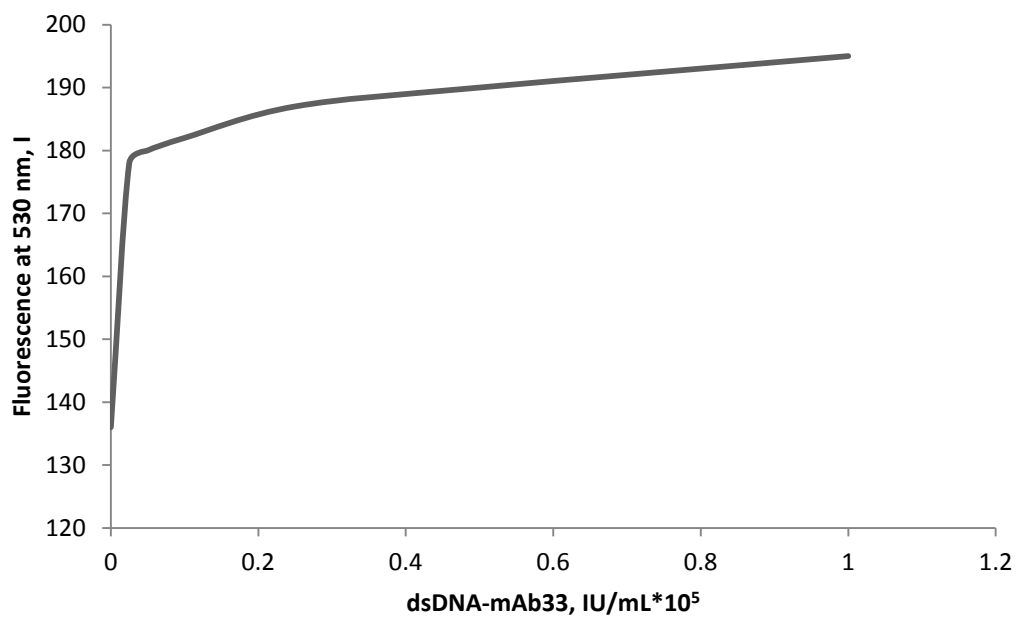


d) **ON8:DNA – mAb33**



Representations of binding modes between fluorescent nucleic acid complexes and proteins used in this study: a) **ON8:DNA** binding BSA, resulting in light-up of fluorescence; b) **ON7:DNA** binding dsDNA-mAb33, resulting in light-up of fluorescence; c) **ON7:DNA** and dsDNA-mAb32 (no binding and no fluorescence signal); d) **ON8:DNA** and dsDNA-mAb33 (no binding and no fluorescence signal). Proteins and nucleic acid complexes are indicated in white and blue, respectively; 5-R110 fluorophores are shown in red, green and white.

Figure S8. Target titration curve for complex ON7:DNA.



Limit of target detection (LOD) values were determined by series of incubations and subsequent analysis of dsDNA-mAb33 at concentrations ($\times 10^5$): 1 IU/mL, 0.5 IU/mL, 0.25 IU/mL, 0.1 IU/mL, 0.05 IU/mL, 0.01 IU/mL, and **ON7**:DNA at concentration 0.5 μ M. Fluorescence intensities were measured at λ^{fl} 530 nm.